

## The Experimental Performance of a Mobile Manipulator Control Algorithm

Norbert A. M. Hootsmans  
Steven Dubowsky  
Patrick Z. Mo  
Department of Mechanical Engineering  
Massachusetts Institute of Technology  
Cambridge, MA 02139 USA

### Abstract

Results are presented of an experimental study of a recently developed motion control algorithm for mobile manipulators. First, the dynamic interactions between a mobile manipulator and its vehicle are shown to lead to poor performance when a conventional fixed-base controller, which neglects these interactions, is used. Then the mobile manipulator control algorithm, which accounts for dynamic vehicle motions caused by manipulator motions, is shown to be stable and to perform well, while using only limited sensory data, such as would be practically available in highly unstructured field environments.

### 1: Introduction

Robotic manipulators are being considered for a wide variety of applications outside of their traditional factory settings. These applications, such as fire-fighting, toxic waste cleanup, and planetary exploration will require the manipulators to operate from moving vehicles, i.e. as mobile manipulators, see Fig. 1 [1].

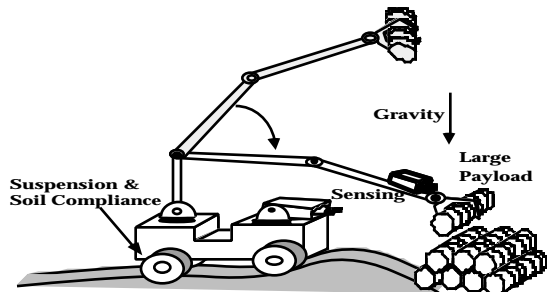


Fig. 1. A Mobile Manipulator Concept.

Typically, a mobile manipulator's vehicle will have significant dynamic behavior, particularly due to suspension compliance, in contrast to factory manipulators generally mounted on rigid bases. As a result, a mobile manipulator's motions will dynamically interact with those of its vehicle on its suspension to degrade the manipulator's performance. Such problems as excessive end-effector errors and poor system stability can result. The control problems for these systems are further exacerbated by highly variable system characteristics due to, for

example, the need to handle a wide range of payloads and to the unknown characteristics of its environment, such as soil characteristics. Finally, the environments for these systems will be unstructured and possibly hostile, which limits the sensing techniques, such as endpoint sensing, that are practically applicable for their control.

The previous research relating to these issues, outlined in Section 2, is limited. However, recently, a method has been developed for the control of large motions of mobile manipulators in unstructured environments, which was shown in planar *simulations*, to provide good nonlinear large motion control [2,3]. This mobile manipulator control algorithm is reviewed in Section 3.1. A full 3-dimensional simulation is presented in Section 3.2 as an example of its expected performance. Furthermore, as previous studies did not consider system stability, it is presented here in Section 3.3. The algorithm is then applied to an experimental system, described in Section 4, and the *experimental* performance of the algorithm is investigated to determine its robustness with respect to unmodelled characteristics of the system, such as sensor delays. The experiments, presented in Section 5.1, show that the algorithm provides good, stable large motion endpoint control for a manipulator mounted on a vehicle with significant compliance, while relying only on easily available base sensory signals of limited quality, rather than on difficult to obtain large motion endpoint sensing. Finally, in Section 5.2, the robustness of this controller to sensor limitations is considered

### 2: Background and prior work

To achieve accurate positioning of a manipulator's end-effector, endpoint control feedback methods have been implemented in various forms [4]. Typically, however, these control algorithms have been applied to robotic manipulators mounted on fixed bases and operating in structured and well known environments. In space robotics research, significant work has been done which considers the dynamic interactions between a manipulator and its spacecraft [5,6]. However, these works assumed systems

with well known characteristics and good sensory information. Further, their performance is not degraded by large disturbances due to gravity and vehicle suspension/tire dynamic characteristics found in terrestrial applications.

A few studies have considered the effects of dynamic interactions between terrestrial mobile manipulators and their vehicles. Some have focused on simulating the system dynamics, but did not consider the problem of controlling the motions of the manipulator with respect to an inertial reference [7,8,9]. Some studies that did consider this issue of control have treated simplified forms of the problem by assuming either a massive vehicle whose motion was unaffected by the manipulator and its payload, or by avoiding vehicle motion with the use of outriggers [10,11]. Fast endpoint feedback has been used to control flexible manipulators and micro-manipulators [12,13]. This approach also has been applied successfully to the problem of mobile manipulator motion control [14]. This study was limited to small planar motions of the manipulator where its endpoint is near its target, thus providing a reference for endpoint sensing. In practice, however, such endpoint sensing will be difficult to achieve along the entire six degree-of-freedom trajectory of large motions of a real manipulator system. Recently, a mobile manipulator control algorithm was developed which does not rely on endpoint sensing, but uses practically available vehicle motion sensors. This approach is called Mobile Manipulator Jacobian Transpose Control (MMJT) [2,3]. The MMJT algorithm was shown to perform well *in simulation*, but to date, the practical utility, including such factors as computational and sensor requirements and robustness with respect to unmodelled system characteristics, has not been studied. The investigation of these issues, which may limit its practical effectiveness, is the focus of the *experimental* study reported on in this paper.

### 3: MMJT control

#### 3.1: The algorithm

The MMJT control algorithm is based on the transpose of a jacobian matrix which relates the manipulator joint velocities and vehicle linear and angular velocities to the linear and angular velocities of the manipulator's end-effector. This matrix is called the Mobile Manipulator Jacobian,  $\mathbf{MMJ}$ . The MMJT algorithm gives the manipulator joint torques,  $\mathbf{m}$ , for an  $n$  degree-of-freedom (DOF) manipulator mounted on a six DOF vehicle with passive suspension as [2]:

$$\mathbf{m} = \tilde{\mathbf{J}}_m^T(\tilde{\mathbf{v}}, \mathbf{q}_m) \mathbf{F}_{edes} + \tilde{\mathbf{G}}_m(\tilde{\mathbf{v}}, \mathbf{q}_m)$$

$$= \mathbf{J}_{fb}^T(\mathbf{q}_m) \begin{bmatrix} \tilde{\mathbf{R}}_v^T(\tilde{\mathbf{v}}) & \mathbf{0} \\ \mathbf{0} & \tilde{\mathbf{R}}_v^T(\tilde{\mathbf{v}}) \end{bmatrix} \tilde{\mathbf{F}}_{edes} + \tilde{\mathbf{G}}_m(\tilde{\mathbf{v}}, \mathbf{q}_m) \quad (1)$$

where  $\mathbf{F}_{edes}$  is a vector of forces and torques reflected to the end-effector. It provides approximate endpoint position and velocity feedback by the following relationship:

$$\tilde{\mathbf{F}}_{edes} = [\mathbf{K}_p] \{ \mathbf{x}_{edes} - \tilde{\mathbf{x}}_e(\tilde{\mathbf{q}}) \} + [\mathbf{K}_d] \{ \dot{\mathbf{x}}_{edes} - \mathbf{MMJ}(\tilde{\mathbf{v}}, \mathbf{q}_m) \dot{\mathbf{q}} \} \quad (2)$$

The symbol “ $\sim$ ” is used above to denote those terms which are only approximately known due to limited vehicle sensing. The vector  $\mathbf{q}$  is composed of the system position coordinates. It contains the vehicle position vector, as well as  $\mathbf{v}$  which represents the vehicle orientation, and  $\mathbf{q}_m$ , the vector of manipulator joint displacements. Recall that the  $\mathbf{MMJ}(\mathbf{v}, \mathbf{q}_m)$  is the Mobile Manipulator Jacobian discussed above. The matrix  $\mathbf{J}_m(\mathbf{v}, \mathbf{q}_m)$  is the sub-matrix of  $\mathbf{MMJ}$  which relates the manipulator joint velocities to endpoint velocities. It can be written as the multiplication of the matrices  $\mathbf{J}_{fb}(\mathbf{q}_m)$  and  $\mathbf{R}_v(\mathbf{v})$ . The matrix  $\mathbf{J}_{fb}(\mathbf{q}_m)$  is the conventional 6 by  $n$  jacobian of an  $n$  DOF fixed-base manipulator, and  $\mathbf{R}_v(\mathbf{v})$  is the 3 by 3 vehicle rotation matrix, dependent only on the vehicle orientation, which relates the vehicle frame to the inertial frame. The vector  $\mathbf{G}_m(\mathbf{v}, \mathbf{q}_m)$  represents the gravity torques acting on the  $n$  manipulator joints. The endpoint position vector  $\mathbf{x}_e(\mathbf{q})$  is calculated using a kinematic model as a function of the system position coordinates  $\mathbf{q}$ .

This algorithm does not rely on difficult to achieve endpoint sensing, but instead uses sensors to measure the vehicle's motion which is combined in a forward kinematic model of the system with the measured manipulator's joint angles to estimate the manipulator's inertial endpoint motions,  $(\tilde{\mathbf{x}}_e, \tilde{\dot{\mathbf{x}}}_e)$ , see Fig. 2. However, in practice, certain vehicle motions (e.g. the yaw motion and the horizontal motions  $z$ ,  $X_v$ , and  $Y_v$ ) would not be easily sensed. These motions will be assumed to be zero; hence the “approximate -  $\sim$ ” terms in Eqs. (1) and (2) and Fig. (2).

#### 3.2: A simulation example

A prototype system, representative of a system that might be designed to perform human scale material handling tasks, was designed in some detail as a baseline for simulation testing of the algorithm [2], see Fig. 3. The system consists of a three DOF 125 kg rigid link hydraulic manipulator with a 25 kg payload mounted on a six DOF four-wheel vehicle. The combined vehicle/manipulator

natural frequencies were modeled as approximately 1 Hz in the vertical direction and 2.5 and 10 Hz in the forward and sideward horizontal directions. The suspension was designed to give

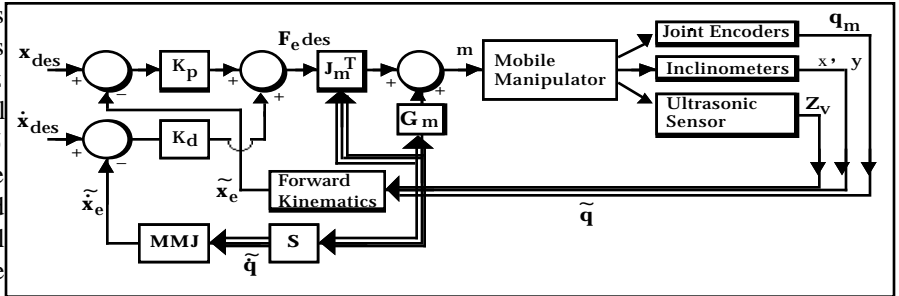


**Fig. 3. Mobile Manipulator Jacobian Transpose Control Block Diagram.**

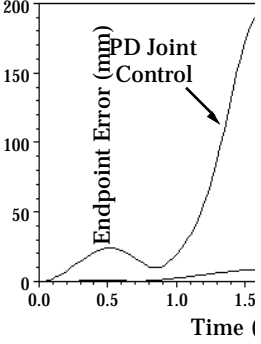


**Fig. 4. Endpoint Errors of MMJT and PD Joint Control Methods.**

damping ratios in the 0.5 - 0.6 range.

A conventional proportional-derivative joint controller was chosen for the manipulator with a 4 to 10 Hz bandwidth and a 1.0 to 2.0 damping ratio, depending on the system configuration. When this controller is used in simulation with a manipulator which is commanded to track a two second straight line trajectory in cartesian space from (0.25 m, 0.45 m, 1.4 m) to (0.05 m, -0.75 m, 0.65 m), see Fig. 3, the manipulator takes more than a second to settle, and the errors are quite large, see Fig. 4.

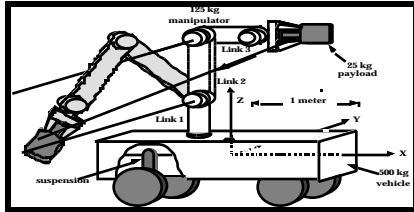


**Fig. 3. A Schematic of A Representative Mobile Manipulator Design.**

These errors are due principally to the interaction of the manipulator and its vehicle, including dynamic, gravity and suspension effects. However, when MMJT control is applied in simulation to the same trajectory, the result is significantly better. The system settles in 0.2 seconds with a maximum dynamic endpoint error of 8.7 mm and a steady state endpoint error of 8.4 mm. Recall that the MMJT controller relies only on limited base sensing in the  $Z_v$ ,  $x$ , and  $y$  directions; the steady state error is due to unmeasured motions in the  $X_v$ ,  $Y_v$  and  $z$  directions. A more detailed summary of the performance of this algorithm predicted by simulations is contained in reference [2]. However, as discussed above the true practical effectiveness of such an algorithm can not be guaranteed by simulation alone. Experimental studies are required, such as discussed below.

**3.2: Stability with complete base sensing**

Although the particular representative system presented in Fig. 3 was found to be quite stable in simulation, the question of general mobile manipulator system stability was investigated in some detail because of the non-colocated architecture of actuation and sensing. It is well-known that if the actuator and sensor of a controller for a flexible system are not located together (non-colocated) the system can exhibit unstable closed loop behavior [15]. Consider the highly-idealized linearized single, rigid-link model of a mobile manipulator, shown in Fig. 5. Here,  $M_m$  is the manipulator mass,  $M_v$  is the vehicle mass,  $k_v$  and  $b_v$  are, respectively, the stiffness and damping of the vehicle suspension.  $A$  is the manipulator actuator, which generates a force  $F$ . The parameter  $b_m$  represents the manipulator joint damping. The variable  $X_m$  denotes the manipulator motion with respect to its vehicle,  $X_v$  is the vehicle motion, and  $X_e$  is the manipulator motion with respect to ground. It is assumed that the manipulator actuation is located at its joint.

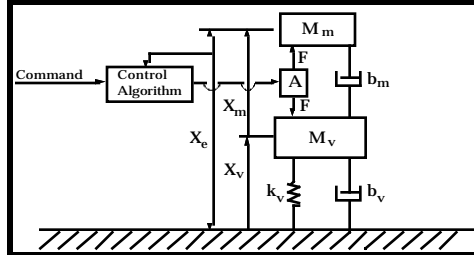


**Fig. 5. Schematic Diagram of a Linearized Single-Link Mobile Manipulator.**

If the manipulator is controlled by measuring only the endpoint position,  $X_e$ , it can be shown that in certain cases instability will occur. A similar result was observed in the endpoint control of micro-manipulators and in endpoint force control [13,16]. Fig. 6 shows the root locus for the system of Fig. 5 for increasing  $k_p$  and constant  $k_d/k_p$ . In this case the mobile manipulator system damping

constants are very low, the manipulator and vehicle have similar mass, and low control gains are used. Clearly there is a range of instability for low system gains. This, however, is an exceptional case. Typically, the vehicle damping,  $b_v$ , will be large enough to prevent instability. In fact, as shown in the root locus plot in Fig. 7, the linearized model of the representative system shown in Fig. 3 is quite stable.

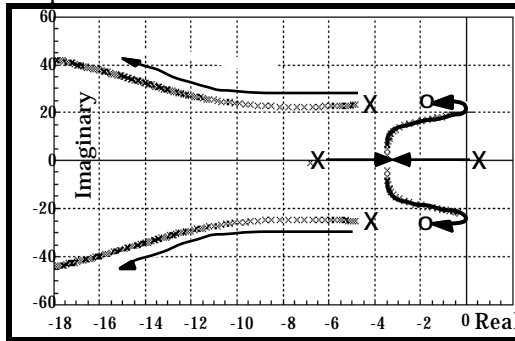


**Fig. 6. Root Locus Showing Instability of an Exceptional MM System.**

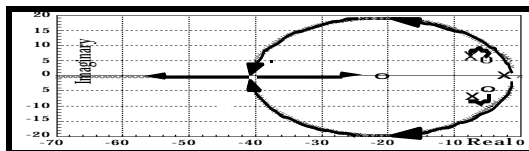


**Fig. 7. Root Locus for Linearized Model of the Representative MM System.**

#### 4: The experimental system

The MMJT control algorithm described above was implemented experimentally on a PUMA 260 experimental manipulator mounted on the MIT Vehicle Emulator System I (VES I) in the MIT Mobile Manipulator Laboratory, see Fig. 8. The VES is a six DOF hydraulically actuated Stewart platform developed for experimental investigation of the behavior of manipulators mounted on compliant or moving bases. The VES operates under admittance control and can experimentally emulate a wide variety of linear and non-linear compliant vehicles [17].

A six DOF force and torque sensor is mounted on top of the platform and underneath the PUMA. It measures the dynamic interactions between the manipulator and its (emulated) vehicle, the Stewart platform. Based on these forces and torques the admittance controller solves a dynamic model of the emulated vehicle to determine the corresponding motion of the vehicle. Using an inverse kinematic model of the platform the required vehicle motions are translated to commands to the Stewart mechanism. Fig. 9 shows typical forces measured by the force sensor which result from the manipulator/vehicle dynamic interactions during a planar manipulator move.

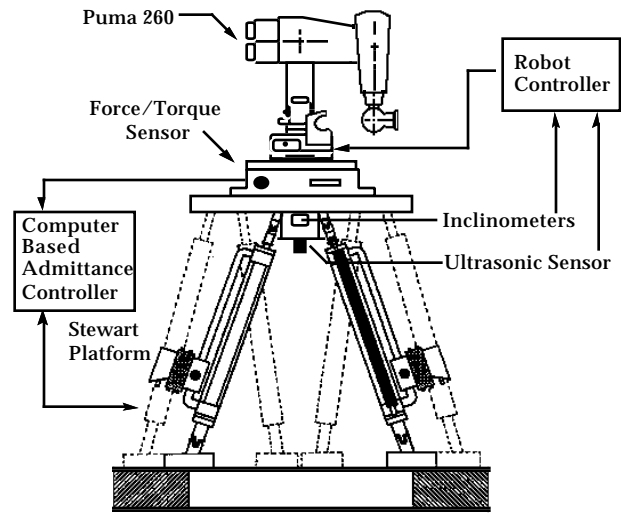


**Fig. 8. The Experimental System Hardware.**

The PUMA manipulator is controlled independently from the Stewart platform by its own micro-computer. As mobile manipulators in unstructured field environments can rely on only limited sensory information, the vehicle sensors were limited to those readily applicable in such environments. Therefore no sensing systems were installed to measure vehicle horizontal displacements and yaw motions. An ultrasonic sensor measures vertical vehicle motion, and two inclinometers measure the pitch and roll angles. These sensor signals provide the manipulator with its only vehicle position and orientation information, as shown earlier in Fig. 2. Both types of sensors are simple, low in cost, and readily available. However, they are both noisy, require filtering, and have considerable time lags and time delays. As discussed earlier, one of the questions to be investigated was whether the control algorithm would tolerate such non-ideal characteristics of vehicle sensors, in addition to the lack of sensing in certain directions. Fig. 10 shows the motion sensed by the ultrasonic sensor and the inclinometer during a planar straight line PUMA move as compared to the actual vehicle motions emulated by the VES.

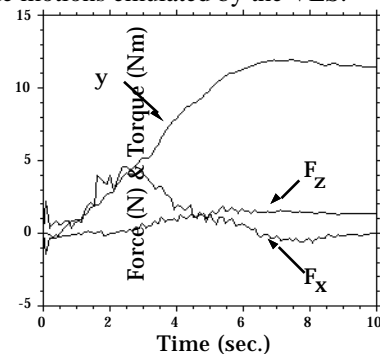


**Fig. 9. The Manipulator/Vehicle Dynamic Interaction Forces.**

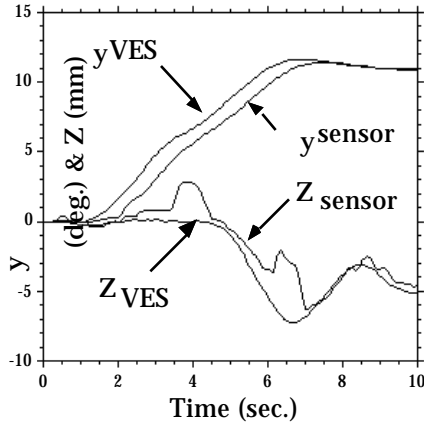


Fig. 10. Performance of Vehicle Sensors.

## 5: Experimental and stability results

### 5.1: MMJT control performance

For this work the VES admittance model was chosen so that the mobile manipulator consisting of the PUMA and its emulated vehicle represented a scaled down version of the system described in Fig. 3. The six DOF PUMA has a mass of approximately 15 kg. The vehicle mass was set to 50 kg, and its suspension characteristics were set to result in a combined vehicle/manipulator natural frequencies of 3 Hz in the vertical direction, 6 Hz in the horizontal direction, and 1.5 - 2 Hz in the rotational direction, depending on the system configuration. Furthermore, damping ratios were set to 0.3 in the vertical direction, 0.6 in the horizontal direction, and to about 0.2 in the rotational direction. Fig. 8 shows the measured manipulator/vehicle dynamic interaction forces when the manipulator was commanded to follow a 5 second, approximately 0.5 meter, straight line planar trajectory. The resulting vehicle motion is shown above in Fig. 10. Clearly the dynamic interaction leads to large vehicle motion. Also, significant inaccuracies and time delays are clearly evident in the sensor signals.

Fig. 11 shows the endpoint performance for the manipulator for the above experiment using both PD joint control and MMJT control. Comparing the desired end-effector path with the actual path followed under the PD control case and the MMJT controller shows clearly that the PD controller gives relatively large errors. These errors are due principally to the motion of the vehicle. Test of the PUMA under PD control with the platform locked, emulating a fixed base, resulted in minimal endpoint errors for this motion. The maximum dynamic endpoint error shown in Fig. 11 for the PD controller is 183 mm and it has a steady state endpoint error of 180 mm. In contrast, the MMJT controller compensates for the vehicle dynamic motion and results in a much smaller maximum dynamic

endpoint error of 18 mm and a steady state endpoint error of 1.7 mm. Recall that the MM controller relies only on the limited vehicle motion information provided by the ultrasonic sensor in the Z-direction, and the inclinometer in the x direction.

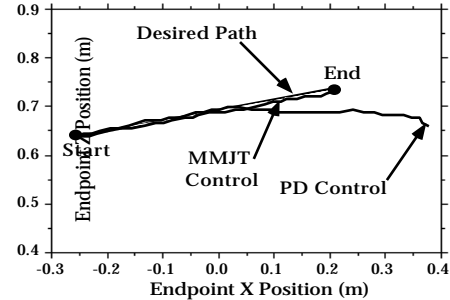


Fig. 11. Endpoint Motion of the MMJT and PD Control Methods.

### 5.3: Robustness to sensor limitations: performance and stability

The experimental results obtained in this study, such as those presented above, demonstrated the ability of the MMJT controller to compensate for manipulator/vehicle interaction and to provide effective and stable large motion endpoint control for a manipulator mounted on a vehicle with significant compliance, despite its reliance on only low cost, readily available, but relatively slow and inaccurate vehicle motion sensors. Given this reliance on vehicle motion sensors, the sensitivity of the system performance and stability to both limited available sensing and sensing errors, such as noise, lag and time delays, was considered in detail and is discussed below.

The absence of certain vehicle sensor signals, while degrading performance, actually tends to stabilize the system. In the limit, with no vehicle sensing, the manipulator motion is controlled with respect to the vehicle as opposed to with respect to inertial space. The system is then no longer non-colocated, and one can argue from passivity theory that the system is inherently stable, by noting that a manipulator controlled stably with respect to its own base will remain stable when mounted on a passive compliant vehicle.

Compared to manipulator joint motion sensors, such as joint encoders, vehicle sensors, such as the ultrasonic sensor and inclinometers, are noisy and slow. The effect of a noisy inclinometer signal on the endpoint error of the manipulator is shown in Fig. 12. The manipulator tries to compensate for a perceived high frequency vehicle vibration, resulting in a jittery endpoint motion. Filtering of the sensor signal results in a graceful motion. However, the filter lag increases the endpoint errors, see Fig. 12.

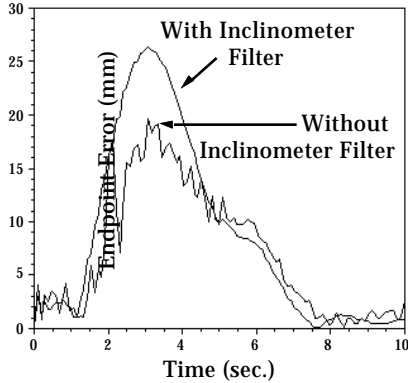


**Fig. 12. Effect of Vehicle Sensor Noise and Filter Lag on Endpoint Motion.**

The effect on stability of the filter lags, or lags in the sensor itself, was investigated using a linearized stability criterion derived from the Routh-Hurwitz stability criterion. However, the result is complex. For systems with good stability characteristics, such as the representative design described above, the system will remain stable even for a very large lag, although its performance will become sluggish, as seen in Fig. 12. However, systems that have poor stability margins, such as presented above in Fig. 6, may become unstable for small lags. However, with increasing lag time they will become stable again. The conclusion is that the effect of sensor and filter lags on system stability is not likely to present serious problems, but should be considered during the design process.

Vehicle sensors such as the ultrasonic distance sensor may also have significant sampling time delays. Fig. 13 shows the effect of vehicle sensor time delay on the manipulator's experimental ability to track its endpoint trajectory. Here the manipulator was commanded to follow its approximately 0.5 meter trajectory in 2.0 seconds. As shown in Fig. 13, the maximum dynamic endpoint error increased from 3.4 mm for a 0.1 sec time delay, to 26.3 mm for 0.6 seconds. This result suggests that even for low performance manipulator systems the effects of time delays can be seen and hence this issue should be considered during the design process.

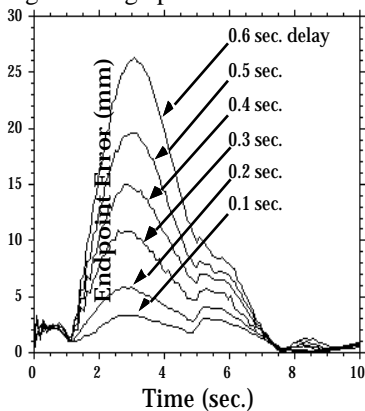


**Fig. 13. Experimental MM Endpoint Error vs. Vehicle Sensor Time Delay.**

Similarly, the absolute accuracy of the vehicle sensors needs to be anticipated in the design of such systems. Fig. 14 shows the effect of sensor errors introduced into the vehicle orientation measurements. This figure clearly shows the direct correlation between the accuracy of the sensor and the manipulator endpoint error.

## 6: Conclusion

Experimental results have shown that dynamic interactions between a mobile manipulator and its vehicle can lead to large manipulator endpoint errors when a conventional fixed-base controller is used, which neglects these interactions. The Mobile Manipulator Jacobian Transpose control algorithm, which accounts for dynamic vehicle motions caused by manipulator motions, was shown to provide good nonlinear large motion control, while using only limited vehicle sensory data, such as would be practically available in highly unstructured field environments. The experimental mobile manipulator system was found to be quite stable, and analytical analysis showed that this is the case for most mobile manipulator systems. An exception arises for systems with low damping constants, with similar vehicle and manipulator masses, and with low control gains. The absence of certain vehicle sensors was shown to degrade system performance, but actually improves stability. Sensor signal noise was shown to lead to undesirable endpoint vibrations, and sensor filters were necessary. Filter lags and lags in the sensor itself were shown to be unlikely to present stability problems, but do decrease system bandwidth. Sensor time delays and accuracy errors were shown to be directly correlated with experimental endpoint errors, and should be considered specifically during the design process of mobile manipulator systems.

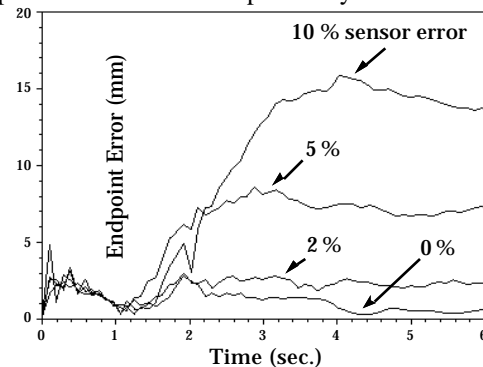


**Fig. 14. Experimental MM Endpoint Error vs. % Inclinometer Error.**

## 7: Acknowledgement

The support of this work by NASA (Langley Research Center, Automation Branch) under Grant NAG-1-801 is acknowledged.

## 8:References

1. Goldsmith, S., "It's a Dirty Job, but Something's Gotta Do It," *Business Week*, August 20, 1990, pp. 92-97.
2. Hootsmans, N.A.M., and Dubowsky, S., "Large Motion Control of Mobile Manipulators Including Vehicle Suspension Characteristics," *Proc. 1991 IEEE Inter. Conf. on Robotics and Auto.*, Sacramento, CA, Apr., 1991 pp. 2336-2341.
3. Hootsmans, N.A.M., and Dubowsky, S., "The Control of Mobile Manipulators Including Vehicle Dynamic Characteristics," *Proc. IV Topical Meeting on Robotics and Remote Systems*, Albuquerque, NM, Feb. 24-28, 1991.
4. Khatib, O., "A Unified Approach for Motion and Force Control of Robot Manipulators: The Operational Space Formulation," *IEEE J. of Robotics and Auto.*, Vol. 3, No. 1, Feb. 1987, pp. 43-53.
5. Hollars, M.G., Cannon, R.H., Jr, Alexander, H.L., and Morse, D.F., "Experiments in Advanced Control Concepts for Space Robotics: An Overview of the Stanford Aerospace Robotics Laboratory," *Proc. of the 10th Annual AAS Guidance and Control Conf.*, Keystone, CO, Jan., 1987.
6. Papadopoulos, E., and Dubowsky, S., "On the Nature of Control Algorithms for Space Manipulators," *Proc. of 1990 IEEE Inter. Conf. on Robotics and Auto.*, Cincinnati, OH, May, 1990, pp. 1102-1108.
7. Wiens, G. J., "Effects of Dynamic Coupling in Mobile Robotic Systems," *Proc. SME Robotics Res. World Conf.*, Gaithersburg, MD, May, 1989, v. 3 pp.43-57.
8. Dubowsky, S., Gu, P-Y, and Deck J. F., "The Dynamic Analysis of Flexibility in Mobile Robotic Manipulator Systems," *Proc. VIII World Congress on the Theory of Machines and Mechanisms*, Prague, Czech., Aug., 1991.
9. Murphy, S.H., Wen, J. T.-Y., and Saridis, G.N., "Simulation of Cooperating Robot Manipulators on a Mobile Platform," *IEEE J. Robotics and Auto.*, v. 7, No. 4, Aug 1991, pp. 468-478.
10. Dubowsky, S., and Tanner, A. B., "A Study of the Dynamics and Control of Mobile Manipulators Subjected to Vehicle Disturbances," *Proc. of the IV International Symposium of Robotics Research*, Santa Cruz, CA, 1987.
11. Dubowsky, S., and Vance, E.E., "Planning Mobile Manipulator Motions Considering Vehicle Dynamic Stability Constraints," *Proc. of the 1989 IEEE Inter. Conf. on Robotics and Auto.*, v. 3, Scottsdale, AZ, May, 1989, pp. 1271-1276.
12. Schmitz, E., *Experiments on the End-Point Position Control of a Very Flexible One-Link Manipulator*, Ph.D. Thesis, Department of Aeronautics and Astronautics, Stanford University, Stanford, CA, April 1985.
13. Sharon, A., *The Macro/Micro Manipulator: An Improved Architecture for Robot Control*, Ph.D. Thesis, Department of Mechanical Engineering, MIT, Cambridge, MA, Sept., 1988.
14. West, H., Hootsmans, N., Dubowsky, S., Stelman, N., "Experimental Simulation of Manipulator Base Compliance," *Proc. of the First Inter. Symp. on Experimental Robotics*, Montreal, Canada, June 1989.
15. Gevarter, W.B., "Basic Relations for Control of Flexible Vehicles," *AAIA Journal*, Vol. 8, No. 4, pp. 666-672.
16. Eppinger, S.D., *Modeling Robot Dynamic Performance for Endpoint Force Control*, Sc.D. Thesis, Department of Mechanical Engineering, MIT, September, 1988.
17. Dubowsky, S., Paul, I. and West, H., "An Analytical and Experimental Program to Develop Control Algorithms for Mobile Manipulators," *Proc. of the VII Symp. on Theory and Practice of Robots and Manipulators*, Sept. 12-15, 1988, Udine, Italy.